TRANSACTIONS
of the
7th International Conference on

STRUCTURAL MECHANICS IN REACTOR TECHNOLOGY

Marriott Hotel
Chicago, Illinois, U.S.A. ■ August 22-26, 1983

Vol. J. Loading Conditions and Structural Analysis of Reactor Containment

Conference organization by:
International Association for Structural Mechanics in Reactor Technology
CEC The Commission of the European Communities
ANL The Argonne National Laboratory

References

1. "Concrete structures under impact and impulsive loading" Proceedings of RILEM-CEB-IABSE-IASS-International Symposium, Bundesanstalt für Materialprüfung (BAM), Berlin (1982)

2. Transactions of the 6th Int. Conf. on Structural Mechanics in Reactor Technology, Paris (1981)

3. "ADINA - A finite element program for automatic dynamic incremental nonlinear analysis" Report 82 448 - 1, MIT (1976)

4. "ASHSD - Dynamic stress analysis of axisymmetric structures under arbitrary loading" Report 69-10, University of California (1969)

Three-Dimensional Non-Linear Aircraft Impact Analysis

J. Marti, G.S. Kalsi
Principia Mechanica Ltd., Newton House, 50 Vineyard Path, London SW14 8ET, U.K.

I. Attalla
Kraftwerk Union AG, Abteilung V591, Postfach 962, D-6050 Offenbach, Germany

SUMMARY

Crude assumptions and computational tools often result in over-conservative and thereby over-expensive designs. The computational power of modern day computers allied with sophisticated analytical techniques should lead to the emergence of better and cheaper designs.

These ideas are considered here in the context of a problem of aircraft impact effects on underground structures. The dynamic and three-dimensional character of these problems cannot generally be neglected. Also, strains tend to be sufficiently large to activate at least constitutive and possibly geometrical non-linearities.

The present paper describes a procedure where full advantage is taken of the possibilities of analysis to assess a design as realistically as possible. The numerical procedure described is fully three-dimensional, dynamic and non-linear. Elastoplastic formulations are used to represent soil, concrete and reinforcing steel, the latter having been incorporated explicitly. Finally, a non-reflecting boundary which cancels wave reflections in the time domain, is introduced to limit the extent of the mesh. The analysis of two sample meshes is briefly discussed. In spite of their relatively large size and complexity, the procedure is such that a minicomputer is sufficient to analyse them.

1. INTRODUCTION

The probability of an aircraft impacting a nuclear power plant is exceedingly small. However, due to the extreme safety which characterises nuclear design, most modern nuclear facilities are assessed for impact from aircraft.

A number of analyses have been published in the recent past dealing with the problem of aircraft impact on nuclear installations. Most of the investigative effort has been concentrated on reinforced concrete structures above the ground surface, particularly the containment building ([1], [2], [3], [4] among others). Of less general applicability is the limited work reported in relation to underground structures ([5], [6]). Although analyses of underground structures subjected to blast loads have often been performed in relation to defence and mining activities, studies of impact effects on underground structures remain scarce.

A significant recent addition to the literature in this general field was afforded by the Berlin Symposium on Concrete Structures under Impact and Impulsive Loading (Plauk [7]).

In the rest of this paper, a methodology is presented for analysing the effects of aircraft impact on underground structures. The procedure described is then applied to an example problem.

2. GENERAL METHODOLOGY

Impact and other short duration problems are often best treated with explicit time-marching procedures, which afford greatest constitutive flexibility and generality of behaviour. The procedure selected is based on a Lagrangian finite difference scheme, the differences being central both in space and time. The methodology presented has been implemented by Marti [8] into PR3D, a commercially available computer program.

The problem requires the solution of two basic sets of equations: the constitutive equations and the momentum equations. The constitutive equations are formulated incrementally and applied explicitly, that is, increments of the stress tensor are computed as a function of strain increments, strains, strain-rates, etc. This relationship is never inverted, thus avoiding the singularities and instabilities which would arise when modelling softening materials or structures. The three-dimensional momentum equations are integrated explicitly on a time-marching basis. This provides greatest generality at the cost of a small integration timestep, a drawback of limited importance in short duration problems.

Solid elements are used in modelling soil and mass concrete. However, the treatment of reinforced concrete presents special difficulties. Reinforced concrete behaviour has been handled here as a combination of individually modelled concrete mass elements and reinforcing bars. The specific constitutive behaviours used for concrete, reinforcing bars and soil are presented in a further section.

Nagtegaal et al [9] have shown that, unless the degrees of freedom per space element exceed the constraints imposed by local incompressibility, an artificial stiffening of the mesh occurs during plastic flow. As a consequence, plastic collapse loads may be grossly overestimated, even for infinitely refined meshes. Equally, it is well known that too many degrees of freedom per element result in the appearance of unrestrained combinations of nodal displacements. This problem is known as 'hourglassing'.

To overcome those problems Marti and Cundall [10] proposed the mixed discretisation scheme, where deviatoric and isotropic parts of the strain and stress tensors are referred to different space discretisations. This procedure has been implemented in the analyses described in this paper. It can be shown [8] that the technique prevents the development of unrestrained hourglassing modes but does allow accurate modelling of plastic flow.

3. FIELD EQUATIONS

As mentioned earlier, two main sets of equations have to be solved: the momentum equations and the constitutive laws. Once space is discretised, each node represents a small volume of material bounded by a surface s. The mass, m, of that volume is lumped at the node. The momentum equations can then be expressed:

$$\ddot{u}_i = \frac{\int_s \sigma_{ij} n_j ds + F_i}{m} + f_i \qquad (1)$$

where u_i are the displacements; σ_{ij} is the stress tensor; n_j is the normal to the surface s; f_i are the body forces; F_i is the resultant of external and structural forces acting at the node; dots imply time derivatives.

The central explicit integration is expressed simply by:

$$\Delta\dot{u}_i = \ddot{u}_i \Delta t$$
$$\Delta u_i = \dot{u}_i \Delta t \qquad (2)$$

where Δt is the integration timestep.

Equations (2) produce velocities and displacements which can be used for continuous updating of the geometry. In the continuum, increments of strains and rotations are computed as:

$$\Delta\varepsilon_{ij} = (\dot{u}_{i,j} + \dot{u}_{j,i})\,\Delta t/2$$
$$\Delta\theta_{ij} = (\dot{u}_{i,j} - \dot{u}_{j,i})\,\Delta t/2 \qquad (3)$$

where ε_{ij} and θ_{ij} are the strain and rotation tensors, respectively; commas indicate derivatives with respect to spatial coordinates.

Similarly, the longitudinal strain in a structural element extending from A to B is:

$$\Delta\varepsilon = \frac{(\dot{u}_i^A - \dot{u}_i^B)(x_i^A - x_i^B)}{|x_i^A - x_i^B|}\,\Delta t \qquad (4)$$

where x_i are the nodal coordinates.

The rotation tensor is required for implementing the Jaumann formulation, which must be used for all variables referred to the Lagrangian frame, in particular the stress and strain tensors. The strain and strain increment tensors are used to enter the constitutive laws.

4. CONSTITUTIVE LAWS

For the problems described in Section 6, concrete is modelled as an elastoplastic solid with limited tensile strength and a criterion to detect crushing. The elastoplastic behaviour has been represented in some cases with a simple bilinear law, while in others smooth non-linear hardening curves have been used.

An elastoplastic law was also used for describing the reinforcing bars. The compressional, bending and shear strength of the bars were neglected. Apart from their elastoplastic behaviour, a fracture criterion based on peak tensile strains was added to the formulation.

The non-linearity of soil behaviour must be taken into account even for relatively small strains. Phenomena such as internal energy dissipation, distortion and dispersion of waves, residual deformations, etc, cannot be properly modelled unless a truly non-linear constitutive law is used. Soil was therefore modelled by means of an elastic non-ideally plastic law, in which the elastic region shrank to the hydrostatic axis. Hence plastic strains are induced from the onset of deformation. The hyperbolic hardening law implemented was considered to depend on the effective confining pressure:

$$\tau_{oct} = \frac{A\varepsilon^p_{oct}}{1 + \frac{A\varepsilon^p_{oct}}{B+C\sigma'}} \qquad (5)$$

where τ_{oct} and ε^p_{oct} are the octahedral shear stress and octahedral plastic shear strain, respectively; σ' is the effective mean stress; A, B and C are material properties.

Although unloading is purely elastic, this is not considered inadequate for studying the response under an aircraft crash loading history.

5. NON-REFLECTING BOUNDARIES

With the purpose of allowing the use of smaller meshes than would be required otherwise, a non-reflecting boundary was implemented. This boundary operates in the time domain and was recently developed by Kunar and Marti [11]. The procedure used is based on the superposition of elastic solutions to two complementary sets of boundary conditions in the vicinity of the non-reflecting boundary. It can be shown that, providing only linear behaviour takes place near the boundary, all elastic reflections will be duly cancelled.

Traditional boundary conditions would have required the boundary to be placed at such a distance that no significant energy would be reflected back to the region of interest. This is an extremely expensive requirement in three-dimensional modelling. The non-reflecting boundary used relaxes this condition in that the boundary need only be just beyond the farthest region where non-linear behaviour is triggered.

Although not discussed in the next section, the influence of the non-reflecting boundaries was quantified by repeating runs with various traditional boundary conditions, as well as with the non-reflecting conditions. This applied to all surfaces across which an infinite mesh would have been desirable. For the examples analysed, the boundary has a significant influence in both stresses and vibration levels. Differences on the order of 10% in the vertical stress, and 30% in vertical accelerations can be considered typical.

6. EXAMPLES

The design loading adopted for representing the aircraft impact corresponds to the time history shown in Figure 1. This loading history is applied on a circular section with an area of $7m^2$.

The generic calculations reported relate to studies conducted on the safety of four underground emergency cooling ducts. The ducts are protected by a surface slab of reinforced concrete 90cm thick with reinforcing bars running parallel and perpendicular to the direction of the ducts. In these analyses, they are further protected by at least 1.45m of controlled fill.

The natural soil and fill were layered, their stiffness increasing with depth. Part of the soil lay above the water table. For soil beneath the water table, the mean effective stress σ' in eq.(5) was assumed to remain constant, as is to be expected from the short duration over which the analysis is conducted. Initial shear moduli A ranged from 1.0 to $5.2\times10^8 N/m^2$ with a Poisson's ratio of 0.45. Densities varied between 1900 and $2400kg/m^3$.

Concrete was assumed to display an initial Young's modulus of $3.4\times10^{10} N/m^2$ and Poisson's ratio of 0.20. Compressive and tensile strengths were assumed to be $3.5\times10^7 N/m^2$ and $2\times10^6 N/m^2$, respectively. The transition from elastic behaviour to deviatoric yield was bilinear or, alternatively, as described by a hyperbolic hardening curve fitted through the initial tangent and the final asymptote. A density of $2500kg/m^3$ was used.

The reinforcing bars had a tensile strength of $4.6\times10^8 N/m^2$ and a

Young's modulus of $2.1 \times 10^{11} N/m^2$. The mass contribution of the reinforcement was neglected. Areal densities of reinforcement of the surface plate ranged from about 15 to $26 cm^2/m$.

Figures 2 and 3 display the deformed meshes 50msec after impact with the displacements having been magnified by a factor of 10. Maximum surface displacements were attained in all cases between 50 and 60msec after the beginning of the impact history. The first analysis (Figure 2) used a mesh of 18210 tetrahedrons, 3964 nodes and 734 structural elements. Although the actual meshes used are made of tetrahedrons, only hexahedrons (each including six tetrahedrons) have been outlined in the plots for easier visualisation. The second impact was studied with 16968 tetrahedral zones, 3786 nodes and 812 structural elements (Figure 3).

As far as the boundary conditions are concerned, the top surface of the meshes was free to move in any direction. The bottom of the meshes was modelled as a non-reflecting boundary, as were other surfaces which would otherwise have needed an infinite mesh in order to eliminate the influence of reflected waves from the area of interest. The curved boundary adjacent to the nuclear reactor was modelled as a sliding 'plane', i.e. free to move within the 'plane' but unable to leave it.

Although longer runs have been performed, those shown here extend only to 70msec, that is, the duration of the impact. Around 2000 timesteps were required to complete 70msec of analysis. Only very limited results can be presented here for reasons of space. The peak slab velocities obtained in these analyses were 1.8 and 1.5m/s, with maximum deflections between 3 and 4cm. Peak vertical velocities at the ducts were 0.47 and 0.32m/s. Some typical response spectra are shown in Figure 4, corresponding to a point at the top of the middle wall of the ducts in Figure 3. Figure 5 shows the time history of vertical stresses at a location in the middle of this vertical wall.

7. CONCLUSIONS

A methodology has been proposed which is suitable for solving general problems in which the three-dimensional nature of the problem cannot be neglected. This methodology is embodied in a commercially available computer program, PR3D. The fairly general constitutive behaviour available within the program has been limited in the examples presented here to the minimum complexity required to represent all major characteristics of the behaviour of reinforced concrete and soil. Further, non-reflecting boundary conditions are available within the program. These help to restrict the dimensions of the numerical model to a fraction of the size necessary if only traditional boundaries were to be used, thus leading to considerable reductions in the costs of three-dimensional analysis.

The methodology described has been used to assess the effects of aircraft impact on a buried structure. The results of the investigation indicate that the response of the structure is well within acceptable limits.

REFERENCES

[1] Constantopoulos, I.V., Vardanega, C. and Attalla, I., 'Dynamic Response to Aircraft Impact of a Reactor Building with Protective Shell on Independent Foundation', 6th SMiRT, Paris, France, August 17-21, 1981, Paper J9/6.

[2] Schnellenbach, G., Stangenberg, F. and Jeschke, G., 'Reduction of Aircraft Impact Induced Vibrations Due to the Nonlinear Behaviour of Reinforced Concrete', 6th SMiRT, Paris, France, August 17-21, 1981, Paper J9/8.

[3] Varpasuo, P. and Kenttala, J., 'The Analysis of the Containment Building for Global Effects of an Aircraft Crash', 6th SMiRT, Paris, France, August 17-21, 1981, Paper J9/10.

[4] Zimmermann, Th., Rebora, B. and Rodriguez, C., 'Aircraft Impacts on Reinforced Concrete Shells', Symp. on Concrete Structures under Impact and Impulsive Loading, Berlin, Germany, June 2-4, 1982, pp.426-440.

[5] Constantopoulos, I.V., Gryspeert, B.J. and Attalla, I. 'Response of Buried Structures to Aircraft Impact', 6th SMiRT, Paris, France, August 17-21, 1981, Paper J9/5.

[6] Marti, J., Kalsi, G.S., Trbojevic, V.M. and Attalla, I., 'Three-Dimensional Dynamic Non-Linear Modelling of Reinforced Concrete under Impact Loads', Symp. on Concrete Structures under Impact and Impulsive Loading, Berlin, Germany, June 2-4, 1982, pp.548-562.

[7] Plauk, G. (editor), Proceedings of the Interassociation Symposium on Concrete Structures under Impact and Impulsive Loading, Berlin, Germany, June 2-4, 1982, BAM.

[8] Marti, J., 'PR3D Documentation Manuals', Principia Mechanica Limited Technical Reports Nos.PR-TN-4.2 to 7.2, December (1981).

[9] Nagtegaal, J.C., Parks, D.M. and Rice, J.R., 'On Numerically Accurate Finite Element Solutions in the Fully Plastic Range', Comp. Meth. in Appl. Mech. Engrg. 4, pp.153-177 (1974).

[10] Marti, J. and Cundall, P.A., 'Mixed Discretisation Procedure for Accurate Modelling of Plastic Collapse', Intl. J. for Anal. Num. Meth. in Geomech., 6 (1), pp.129-140 (1982).

[11] Kunar, R.R. and Marti, J., 'A Non-Reflecting Boundary for Explicit Calculations', Winter Ann. Meet. Amer. Soc. Mech. Eng. Computational Methods for Infinite Domain Media-Structure Interaction, Washington D.C., November 15-20, 1981, pp.183-204.

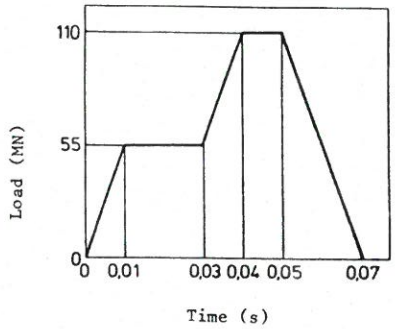

Fig. 1. Load-time history used for analysis

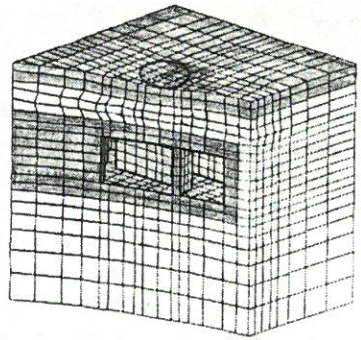

Fig. 2. Deformed shape at 50ms, example 1

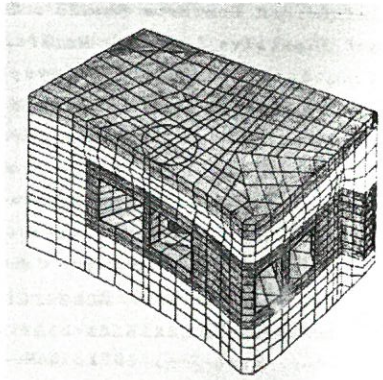

Fig. 3. Deformed shape at 50ms, example 2

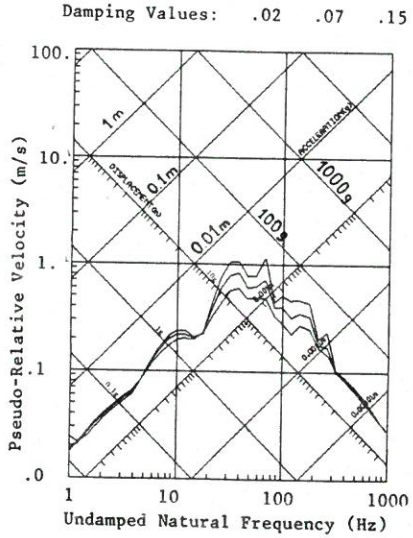

Fig. 4. Typical response spectra plot

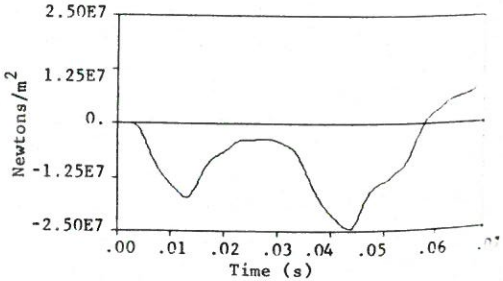

Fig. 5. Typical time-history plot of vertical stress